

SYNTHESIS OF RADAR ABSORBING MATERIALS FOR STEALTH AIRCRAFT BY USING NANOMATERIALS AND EVOLUTIONARY COMPUTATION

Davide Micheli*, Roberto Pastore, Antonio Vricella, Ramon Bueno Morles, Mario Marchetti

**University Sapienza of Rome, Department of Astronautics, Electric and Energy Engineering,
Via Salaria 851, Rome, (Italy)**

Keywords: *Radar absorbing material, frequency selective material, synthesis*

Abstract

The present research shows a powerful method for the design of multi-layered radar absorbing materials useful in low observable and stealth manned or unmanned aircraft systems. The imitation of a desired behavior of the reflection coefficient allows to modeling the optimal arrangement of each layer in terms of material and thickness. A significant enhancement of the electromagnetic absorption is obtained through the use of different kind of carbon nanomaterials uniformly dispersed within an epoxy matrix. Several carbon-based nanocomposite materials are dielectrically characterized in the frequency range 2-18 GHz, and an evolutionary algorithm is used to run the mathematical model in order to find out the optimal solution in terms of the multi-layer composition. Interesting applications of the proposed design method are suggested other types of military targets in the marine and terrestrial scenario where the reduction of the radar observability is mandatory.

1 General Introduction

In the last 60 years the evolution of radar absorbing materials (RAM) [1-4] allowed to reduce the radar detection of military targets. In particular, the geometrical shape and the materials adopted are the main actors in stealth fighters and low observable aircrafts. The goal is to reduce the radar cross section [4] of the

target. The frequency of the detecting radar is one of the main issues in RAM design. In fact, the lower the frequency, the higher are generally the RAM's thickness and mass needed to accomplish the electromagnetic (EM) absorption requirements. Moreover, such parameters must be carefully taken into account because they are potentially in conflict with the aerodynamics and payload capability of the aircraft. Radar systems work in a wide band of transmitted frequencies. The higher the frequency of a radar system, the more it is affected by weather conditions such as rain or clouds. But the higher the transmitted frequency, the better is the accuracy of the radar system. At low frequency, radars are able to detect the target at great distances but with poor capability in recognizing the target details, i.e. the airplane topology and its potential harmfulness. At high frequencies radars are able to provide more details, but at short distances [4]. Nowadays, employed stealth technologies have not the desired effect at extremely low frequencies (below 300 MHz). The most used frequencies are in the bands above 2 GHz up to 18 GHz.

In stealth technology the requirement is a wideband radar invisibility. In low observability technology the condition is less stringent, since it is restricted to reduce the radar detection at short distances, mainly in the frequency range 8-12 GHz. In low observability technology the target is detected at long distance but with few details. When the target gets at shorter distance,

the radar is no more able to detect it since the low reflectivity determines a like noise-floor response. In turns, higher frequencies allow to design thinner and lighter RAM, which is essential for aircrafts. In Table 1 the NATO electronic warfare (EW) RF band designations are reminded, while in Table 2 the frequency bands and the radar operational propagation limitations [5] are reported.

Table 1: NATO Electronic Warfare (EW) RF Band Designations

Radar Designation	ITU Designation	IEEE Designation	Wireless Bands
HF 3-30MHz	HF 3-30MHz	A 0-250MHz	
Not designated	VHF 30-300MHz		
P 216-450MHz	UHF 300-3000MHz	B 250-500MHz	802.15.4
Not designated		C 500 – 1000MHz	
L 1-2GHz		D 1-2GHz	
S 3-4GHz		E 3-3GHz	
C 3-8GHz	SHF 3-30GHz	F 3-4GHz	802.11a, 802.11k
		G 3-6GHz	
		H 6-8GHz	
X 8-12.4GHz		I 8-10GHz	
J / Ku 12.4 – 18GHz		J 10-20GHz	
		K 18-26.5GHz	
Q / Ka 26.5 - 40GHz	EHF 30-300GHz		

In G- Band there are many mobile military battlefield surveillance, missile-control and ground surveillance radar sets with short or medium range. The size of the antennas provides for excellent accuracy and resolution. The influence of bad weather conditions is very high. Therefore, air-surveillance radars often use an antenna feed with circular polarization. This frequency band is predetermined for most types of weather radar used to locate precipitation in temperate zones like Europe.

In I/J (X- and Ku- Band radar) frequency-band (8 to 18 GHz) the relationship between wavelength and antenna size is considerably better than in lower frequency-bands. The I/J-Band is a relatively popular radar band for military applications like airborne radars for performing the roles of interceptor, fighter, and attack of enemy fighters and ground targets. A very small antenna size provides good performances. Missile guidance systems at I/J-Band are of convenient size and are, therefore, of interest for applications where mobility and light weight are important, and where a very long range is not a major requirement. This frequency band is widely used for maritime civil and military navigation radars. Very small and cheap antennas with high rotation speed are adequate for fair maximum ranges and good accuracy. Slotted waveguides and small patch antennas are used as radar antennas, mostly under protective radomes. This frequency band is also popular for spaceborne or airborne imaging radars based on synthetic aperture radar (SAR), both for military electronic intelligence and civil geographic mapping. A special inverse synthetic aperture radar (ISAR) is in use as a maritime airborne instrument for pollution control.

In the K- Band (K- and Ka- Band radar), the higher the frequency, the higher is the EM waves atmospheric absorption and attenuation. Otherwise, the achievable accuracy and the range resolution rise too. Radar applications in this frequency band provide short range, very high resolution and high data renewing rate.

Table 2: Frequency Bands and Radar Operational Propagation Limitations

LF 30–300 kHz	Allocations are provided in the frequency range but no radar usage or applications have been identified.
MF 300–3000 kHz	Used by continuous wave (CW) radar systems for accurate position location. Very high noise levels are characteristic of this band.
HF 3–30 MHz	Refractive properties of the ionosphere make frequencies in this band attractive for long-range radar observations of areas such as over oceans at ranges of approximately 500–2000 nautical miles. Only a few radar applications occur in this frequency range because its limitations frequently outweigh its advantages: very large system antennas are needed, available bandwidths are narrow, the spectrum is extremely congested with other users, and the external noise (both natural noise and noise due to other transmitters) is high.
VHF 30–300 MHz	For reasons similar to those cited above, this frequency band is not too popular for radar. However, long-range surveillance radars for either aircraft or satellite detection can be built in the VHF band more economically than at higher frequencies. Radar operations at such frequencies are not affected by rain clutter, but auroras and meteors produce large echoes that can interfere with target detection. There have not been many applications of radar in this frequency range because its limitations frequently outweigh its advantages.
UHF 300–3000 MHz	Larger antennas are required at the lower end than at the upper end of the UHF band. As compared to the above bands, obtaining larger bandwidths is less difficult, and external natural noise and weather effects are much less of a problem. At the lower end, long-range surveillance of aircraft, spacecraft, and ballistic missiles is particularly useful. The middle range of this band is used by airborne and spaceborne SAR's. The higher UHF end is well suited for short to medium-range surveillance radars. □
SHF 3 GHz–30 GHz	Smaller antennas are generally used in this band than in the above bands. Because of the effects of atmospheric absorption, the lower SHF band is better for medium-range surveillance than the upper portions. This frequency band is better suited than the lower bands for recognition of individual targets and their attributes. In this band, Earth observation efforts employ radars such as SAR's, altimeters, scatterometers, and precipitation radars .
EHF 30–300 GHz	It is difficult to generate high power in this band. Rain clutter and atmospheric attenuation are the main factors in not using this frequency band. However, Earth observation efforts are made in this band employing radars such as altimeters, scatterometers, and cloud profile radars.

These radar sets are called surface movement radar (SMR) or airport surface detection equipment (ASDE). Using of very short transmitting pulses (few nanoseconds) affords a range resolution so that outlines of the aircraft can be seen on the radars display [6].

In this research the attention has been focused on RAMs able to absorb the EM waves in extended or in well selected frequency ranges. In particular, the EM properties of layered structures made of carbon based nanocomposite materials have been studied in the frequency range 2–18 GHz. By taking into account the dielectric parameters of these materials, and by using an appropriate mathematical model, the EM reflection coefficient (RC) at the first air-RAM interface has been simulated.

The layered RAM optimization has been addressed by searching the most appropriate layering of nanocomposite materials able to fit the simulated RC to an a priori established reflection coefficient target (RCT) profile. The concept of frequency selective material (FSM) is introduced recalling that of frequency selective surface (FSS) [7-11]. The entire optimization procedure was managed by an evolutionary algorithm able to link the mathematical model to a database of nanocomposite materials arrayed in terms of their dielectric permittivity. The optimization procedure consists in the minimization of an objective function (OF) which essentially matches the simulated RC with a desired RCT. As far as the background is concerned, a huge amount of papers on RAM can be found in the literature [12-36]: some of the most recent works employ evolutionary algorithms, but none of them makes use of a synthesis method like that proposed in the present research. In section II the materials employed and their dielectric characterization are described. In section III the mathematical model and the optimization algorithm are analyzed. In section IV the results obtained by the simulations of several optimized multilayered structures are presented and discussed.

2 Experimental: nanocomposites characterization

The carbon-reinforced nanocomposite materials are briefly presented. The composite matrix employed is the Tencate EX-1545. It is a 2-part highly modified tough Cyanate Ester resin formulated to have extremely low viscosity at room temperature. The low viscosity allows resin transfer molding (RTM) processing with minimal heat to the resin, which extends resin pot life and mold filling time for difficult and/or large RTM structures. Typical applications of Tencate EX-1545 are

- aircraft structures
- radomes and antennae
- low observables
- missile structures
- high performance and high heat commercial applications

Industrial grade multi walled carbon nanotubes (MWCNT) were employed: they are the Nanocyl™ NC 7000 (average diameter around 9.5 nm, average length 1.5 μm, carbon purity 90%, metal oxide 10%, surface area 250-300 m²/g) supplied by Nanocyl. As reported in the NC 7000 technical datasheet, the volume resistivity (ohm·cm) and the surface resistivity (ohm·sq) of NC 7000 MWCNT-reinforced polymeric composites decrease from 10¹⁵ and 10¹³ to 10³ and 10² respectively when the inclusion weight percentage increases from 0% to 3%. In addition, three more typologies of carbon-based micro/nanoparticles, namely carbon nanofibers (CNF), graphite nanoplatelets (GNP) and polyaniline (PANI), have been investigated in terms of their capability to affect the EM properties of the polymeric matrix. The CNFs were purchased at Sigma Aldrich: they are cylindrical nanostructures with graphene layers arranged as stacked cones, cups or plates. Due to their high electrical conductivity and high aspect ratio, the CNFs can impart equivalent electrical conductivity to a composite at lower loadings than conventional conductive fillers do. The GNPs were provided by XG Sciences (xGNP C-750): they are unique nanoparticles consisting of short stacks of graphene sheets having a platelet shape, now

becoming increasingly available. The GNPs are very thin flat particles (1-20 nm in thickness) with large diameters (1-50 μm). PANI emeraldine base powder with conductivity value of 4-6 S/m and 2-3 μm of particle size was purchased at Sigma Aldrich. PANI is a conducting polymer of the semi-flexible rod polymer family. Some scanning electron microscope (SEM) micrographs of the materials employed are reported in Fig. 1 while in Table 3 their morphological properties are summarized.

Table 3. Main physical characteristics of the carbon-based powder employed.

Carbon Material (wt%)	Dimension	Specific Surface Area (m ² /g)	Aspect Ratio (L/D)
MWCNT (0.5 ÷ 2.0)	av. diameter 9.5 nm av. length 1.5 μm	250 ÷ 300	~ 150
CNF (0.5 ÷ 3.0)	inner diameter 0.5-10nm outer diameter 80-200nm length 0.5-20μm	~ 60	10 ÷ 100
GNP (0.5 ÷ 3.0)	diameter 1-50μm platelet thickness 1-20nm	750	-
PANI (0.5 ÷ 2.5)	particle size 2-3μm	-	-

These carbon-based powders have been mixed in several wt% to the hosting polymeric matrix. A full description of the carbon nanocomposites processing is provided by the authors in previous works [37-43]. The materials have been dielectrically characterized in terms of electric permittivity by means of a vector network analyzer (Agilent PNA-L N5235) and a coaxial airline [38]. The results of the measurement of the electric permittivity have been used to design the multilayered electromagnetic wave absorbers. In Fig. 2 the real and imaginary part of the relative electric permittivity of MWCNT-reinforced composites are shown. A complete report of all the carbon nanocomposite materials realized has been recently published [43]. From the plot of Fig. 2, it can be observed that an increase of the nanomaterials weight concentration determines higher values of the relative electric permittivity.

SYNTHESIS OF RADAR ABSORBING MATERIALS FOR STEALTH AIRCRAFT BY USING NANOMATERIALS AND EVOLUTIONARY COMPUTATION

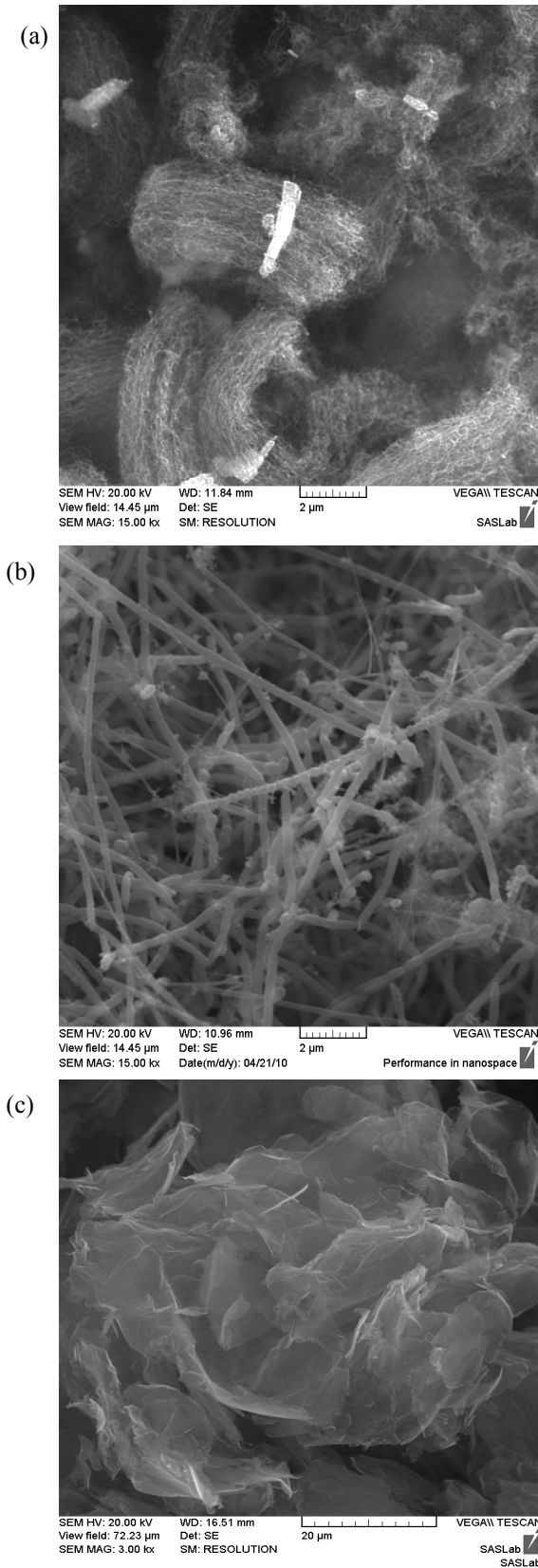


Fig. 1. SEM images of carbon nanostructures: (a) MWCNT, magnification 15 kx; (b) CNF, magnification 15 kx; (c) GNP, magnification 3 kx.

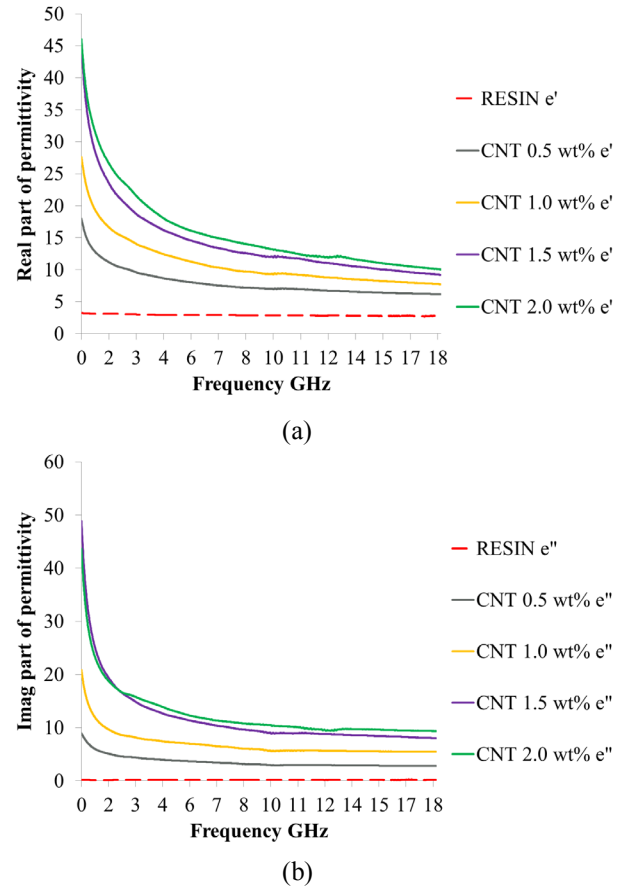


Fig. 2. Relative electric permittivity of MWCNT-reinforced composites: (a) real part, (b) imaginary part in the frequency range 300 MHz-18 GHz.

The possibility to join the most appropriate value of thickness with material type for each layer provides a full capability to design whatever kind of RAM. As one can guess, there are a lot of possible combinations: consequently, an upper limit has been imposed for the thickness of each layer and an iterative optimization approach has been used to the RAM design.

3 Design method

Each nanocomposite material has been coded to provide an univocal identification within the database:

- 1 → Resin Tencate EX-1545
- 2 → MWCNT 0.5wt.%
- 3 → MWCNT 1.0wt.%
- 4 → MWCNT 1.5wt.%
- 5 → MWCNT 2.0wt.%
- 6 → CNF 0.5wt.%

7 →	CNF 1.0wt.%
8 →	CNF 1.5wt.%
9 →	CNF 2.0wt.%
10 →	CNF 2.5wt.%
11 →	CNF 3.0wt.%
12 →	PANI 0.5wt.%
13 →	PANI 1.0wt.%
14 →	PANI 1.5wt.%
15 →	PANI 2.0wt.%
16 →	PANI 2.5wt.%
17 →	GNP C750 0.5wt.%
18 →	GNP C750 1.0wt.%
19 →	GNP C750 1.5wt.%
20 →	GNP C750 2.0wt.%
21 →	GNP C750 2.5wt.%
22 →	GNP C750 3.0wt.%

A set of 22 different materials is thus available to build whatever FSM made of a certain number of layers, able to imitate a desired RCT profile. The search / evolutionary algorithm adopted to minimize the objective function must be able to easily go away from local minima. In this research, particle swarm optimization (PSO)[38], winning particle optimization (WPO)[42] and genetic algorithm (GA)[35,39] were used. Between these tools, as far as the authors experience is concerned, PSO seems to be able to find optimal solutions, minimizing the number of layers and the overall thickness of the FSM better than GA and WPO.

3.1 Mathematical model and layering optimization algorithm

The mathematical model of the multilayer structure has been already published [43]. It takes into account the dielectric parameters of each layer. The material of each layer is set by the iterative optimization algorithm by minimizing the final value of the objective function. The mathematical model and the iterative optimization algorithm can basically work in two main ways: one operates the absolute RC minimization in a desired frequency range [42], the other instead optimizes the RC by following a desired RCT profile [43]. In Fig. 3 two simple examples of expected results are depicted.

The expressions of the objective functions OF_s able to perform the optimization

$$OF_1 = \min \left\{ \sum_f RC(f) \right\} \quad (1)$$

$$OF_2 = \min \left\{ \sum_f \frac{[RC(f) - RCT(f)]^2}{[RC(f) + RCT(f)]^2} \right\} \quad (2)$$

(where f is the frequency step in the range considered) are extensively explained in [43].

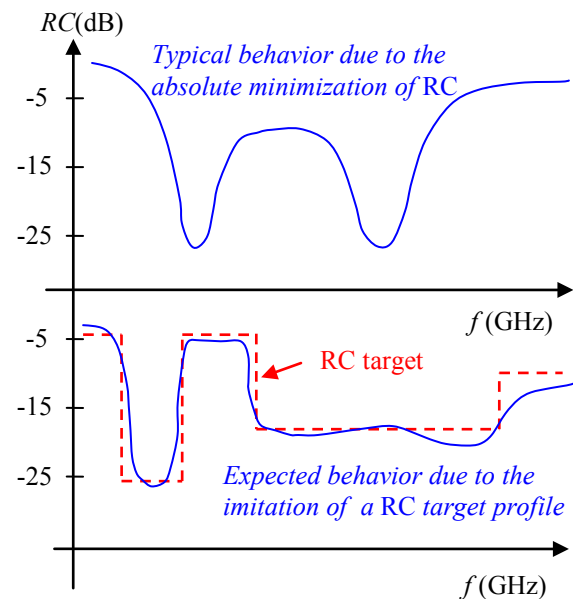


Fig. 3. Typical and expected behavior of the RC curves in the layered RAM optimization by using iterative optimization algorithms. Above, the RC curve is an example of typical result of the absolute minimization of the RC function. Below, the expected RC profile obtained by fitting a RCT is shown.

4 Results

4.1 RC absolute minimization (OF_1)

In this section some results obtained by using OF_1 are shown. Table 4 shows five RAM simulations. The growing thickness of RAM is controlled by a parameter within the OF_1 able to weight the overall thickness vs the EM absorption.

SYNTHESIS OF RADAR ABSORBING MATERIALS FOR STEALTH AIRCRAFT BY USING NANOMATERIALS AND EVOLUTIONARY COMPUTATION

Table 4. RAM simulations using OF_1 .

RAM Simulation	Materials and layers	Thickness of layers (mm)	Total Thickness (mm)
RAM n°1 (Fig. 4)	MWCNT 2.0wt% MWCNT 1.5wt% MWCNT 0.5wt% (PEC)	0.33 0.17 1.43	$\cong 1.94$
RAM n°2 (Fig. 5)	CNF 3.0wt% (PEC)	2.03	$\cong 2.00$
RAM n°3 (Fig. 6)	PANI 2.5wt% MWCNT 2.0wt% MWCNT 1.0wt% (PEC)	3.0 0.14 2.01	$\cong 5.15$
RAM n°4 (Fig. 7)	Resin MWCNT 0.5wt% MWCNT 1.5wt% MWCNT 2.0wt% (PEC)	2.93 2.21 0.65 2.55 7.11	$\cong 8.36$
RAM n°5 (Fig. 8)	PANI 2.0wt% MWCNT 0.5wt% PANI 2.0wt% MWCNT 1.0wt% MWCNT 0.5wt% MWCNT 2.0wt% CNF 2.0wt% CNF 3.0wt% (PEC)	3.5 1.6 0.7 3.2 3.9 1.5 0.1 0.4	$\cong 14.9$

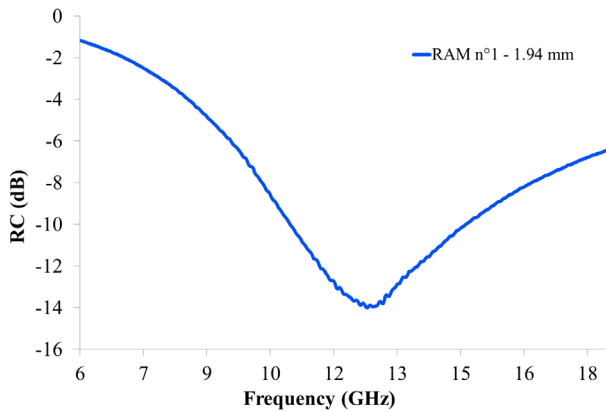


Fig. 4. RAM n°1 thick 1.94 mm, obtained with OF_1 . Frequency range 6-18 GHz.

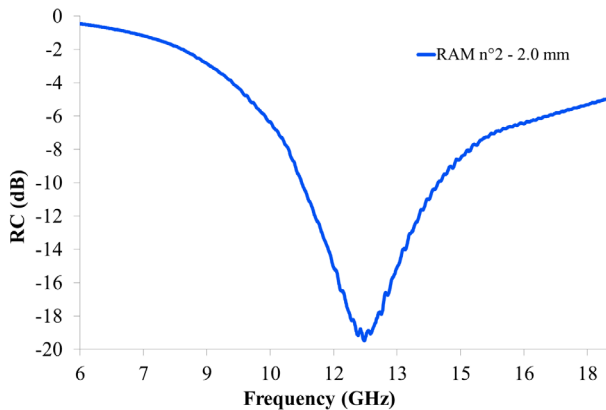


Fig. 5. RAM n°2 thick 2.0 mm, obtained with OF_1 . Frequency range 6-18 GHz.

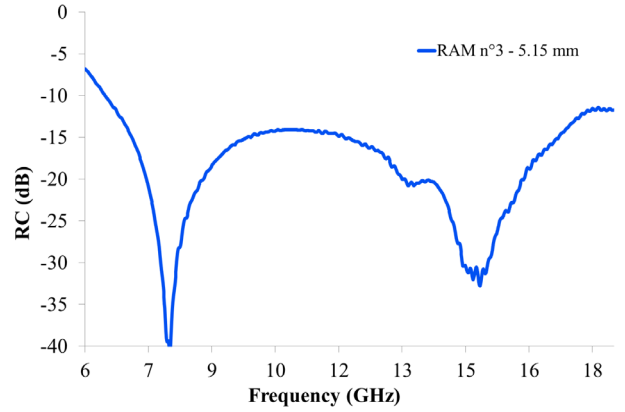


Fig. 6. RAM n°3 thick 5.15 mm, obtained with OF_1 . Frequency range 6-18 GHz.

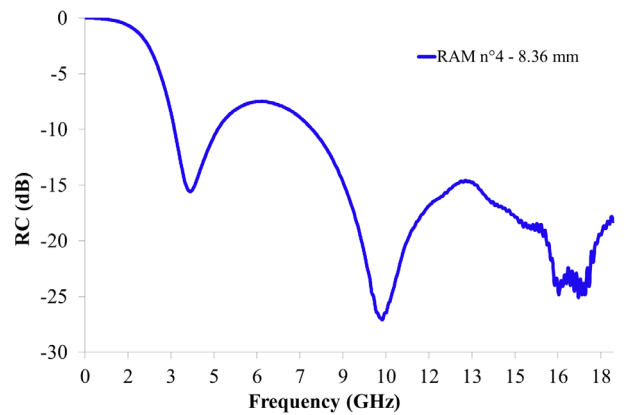


Fig. 7. RAM n°4 thick 8.36 mm, obtained with OF_1 . Frequency range 300 MHz-18 GHz.

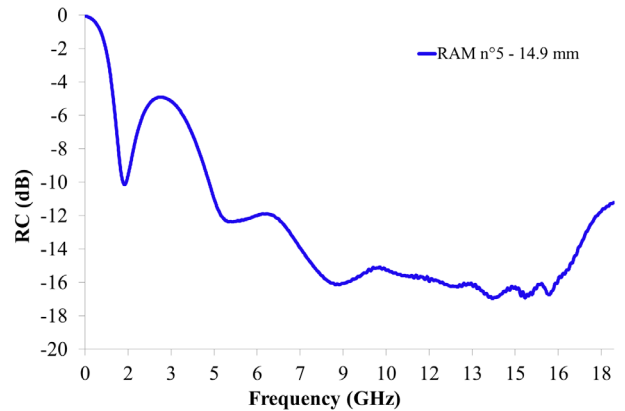


Fig. 8. RAM n°3 thick 14.9 mm, obtained with OF_1 . Frequency range 300 MHz-18 GHz.

By observing the results, it's clear that the minimization of OF_1 does not allow to decide in advance the frequency where the RC will assume the relative minimum values. By increasing the thickness of RAM the absorption bandwidth increases too, but this method lacks EM absorption frequency optimization. The next paragraph deals with such issue.

4.2 Frequency selective optimization (OF₂)

The layering and the EM performance of five RAMs synthesized by applying OF₂ are shown. Table 4 reports materials and layers thickness for each RAM optimized as FSM (i.e., to follow a specific RCT).

Table 4. RAM simulations using OF₂.

RAM Simulation	Materials and layers	Thickness of layers (mm)	Total Thickness (mm)
RAM n°6 (Fig. 9)	GNP 0.5wt% MWCNT 1.5wt% CNF 3.0wt% GNP 2.0wt% MWCNT 1.5wt% PANI 2.0wt% (PEC)	3.80 0.27 1.09 0.21 5.99 3.52	≅ 14.9
RAM n°7 (Fig. 10)	MWCNT 2.0wt% MWCNT 0.5wt% Resin MWCNT 2.0wt% (PEC)	0.20 0.20 1.10 1.40	≅ 2.9
RAM n°8 (Fig. 11)	PANI 0.5wt% CNF 2.5wt% MWCNT 2.0wt% PANI 2.5wt% MWCNT 2.0wt% PANI 1.0wt% MWCNT 2.0wt% CNF 1.0wt% GNP 0.5wt% CNF 2.0wt% (PEC)	3.43 0.98 1.00 0.42 0.83 8.00 1.16 1.36 5.10 6.53	≅ 28.8
RAM n°9 (Fig. 12)	GNP 0.5wt% CNF 1.0wt% MWCNT 2.0wt% CNF 3.0wt% PANI 1.0wt% (PEC)	3.25 7.74 3.32 0.59 5.69	≅ 20.6
RAM n°10 (Fig. 13)	CNF 1.5wt% CNF 3.0wt% CNF 2.5wt% MWCNT 1.5wt% PANI 0.5wt% CNF 1.5wt% (PEC)	3.49 1.68 0.56 9.00 2.88 1.44	≅ 19.0

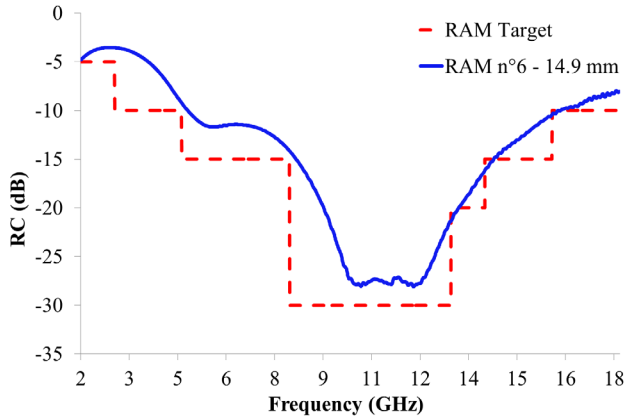


Fig. 9. RAM n°6 thick 14.9 mm, obtained with OF₂. Frequency range 2-18 GHz.

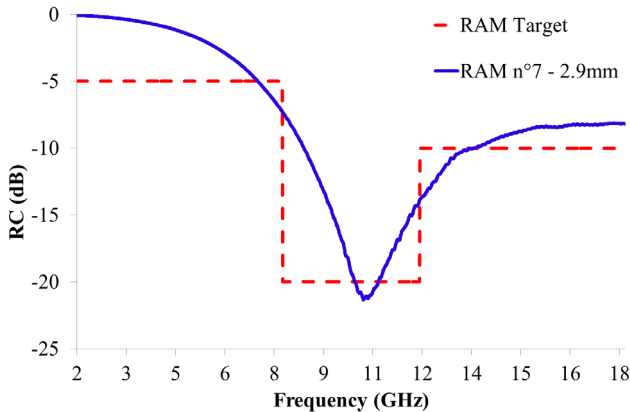


Fig. 10. RAM n°7 thick 2.9 mm, obtained with OF₂. Frequency range 2-18 GHz.

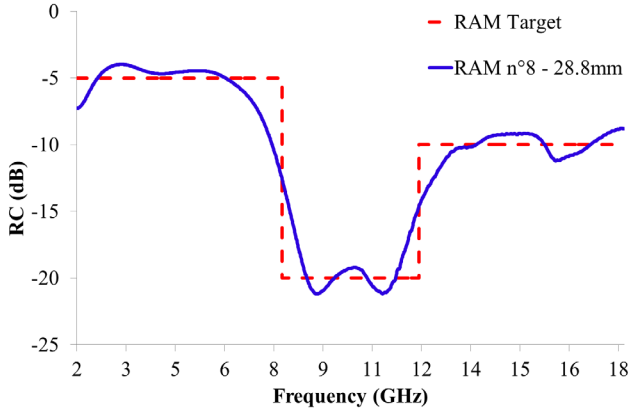


Fig. 11. RAM n°8 thick 28.8 mm, obtained with OF₂. Frequency range 2-18 GHz.

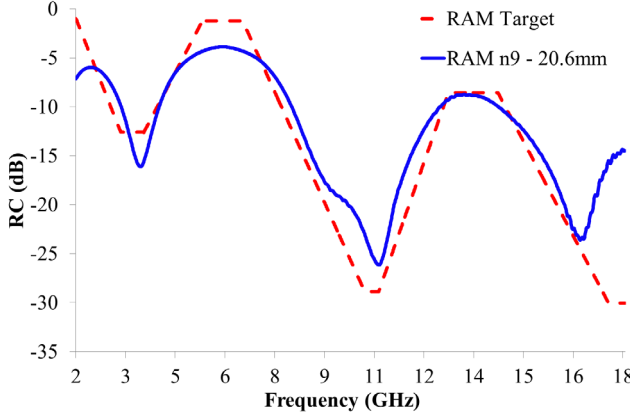


Fig. 12. RAM n°9 thick 20.6 mm, obtained with OF₂. Frequency range 2-18 GHz.

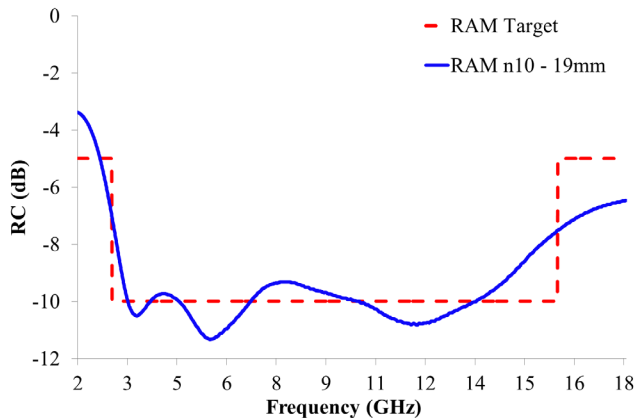


Fig. 13. RAM n°10 thick 19 mm, obtained with OF₂. Frequency range 2-18 GHz.

By observing the plots obtained minimizing OF₂, it can be highlight the possibility to synthetize every kind of RC response. Such result is particularly important for applications of radar signature reduction in predefined frequency band, as reported in Tables 1,2.

The last result shown in Fig. 13 is quite interesting for extended absorption bandwidth applications. The thicknesses of the synthetized RAMs reported in Table 4 could appear inapplicable in some real scenarios where the maximum allowed thickness is of few mm. Nevertheless, it must be taken into account that by adding other kind of nanomaterials to the database, the EM losses of basic nanocomposites could be enhanced, thus allowing to reduce the thickness of the single layers and of the final RAM.

5 Conclusion

In this work a methodology for multilayered RAM design by using the “synthesis” approach is described. This method need to access to an existing database of materials. Each material can be properly selected for a RAM layer. The materials in the database finally determine the RAM thickness and set the constraints which allow the synthesis to be successful in imitate a desired RC profile. The obtained results suggest this method as effective route to design advanced RAMs for military applications where FSMs seem to be the key to optimize the radar signature suppression performances. The

present research shows a powerful method for the design of multi-layered radar absorbing materials useful in low observable and stealth manned or unmanned aircraft systems.

References

- [1] Sheffield RG. *The official F-19 stealth fighter handbook*. Radnor, Pennsylvania: Pam Williams; 1989.
- [2] Mosallaei H, Rahmat-Samii Y. RCS reduction of canonical targets using genetic algorithm synthesized RAM. *IEEE T Antenn Propag*;48(10):1594-606, 2000.
- [3] Vinoy KJ, Jha RM. *Radar Absorbing Materials - From Theory to Design and Characterization*. Boston, MA: Kluwer; 1996.
- [4] Knott EF, Shaeffer J, Tuley M. *Radar Cross Section. 2nd ed.* Raileigh, NC: SciTech Publishing, Inc.: 7-11, 2004.
- [5] Manual of Regulations and Procedures for Federal radio Frequency Management. “Rebook”, “NTIA Manual”. <http://www.ntia.doc.gov/osmhome/redbook/redbook.html>
- [6] Merrill Skolnik. *Radar Handbook, Third Edition*. January 22, 2008 | ISBN-10: 0071485473 | ISBN-13: 978-0071485470, 2008.
- [7] Costa F., Monorchio A., Manara G. Analysis and Design of Ultra Thin Electromagnetic Absorbers Comprising Resistively Loaded High Impedance Surfaces. *Antennas and Propagation, IEEE Transactions on*; 58: 1551-1558, 2010.
- [8] Y. El-Kahlout and G. Kiziltas. Inverse synthesis of electromagnetic materials using homogenization based topology optimization. *Progress In Electromagnetics Research*; 115: 343-380, 2011.
- [9] Hofer, W.J.R. Time reversal and optimal electromagnetic structure synthesis. *Electromagnetic Theory (EMTS), URSI International Symposium on 2010*: 287 – 290, 2010.
- [10] Chiya Saeidi and Daniel van der Weide. Synthesizing frequency selective metasurfaces with nanodisks. *Appl. Phys. Lett.*; 103, 2013.
- [11] Agostino Monorchio, Giuliano Manara, Luigi Lanuzza. Synthesis of Artificial Magnetic Conductors by Using Multilayered Frequency Selective Surfaces. *Antennas and Wireless Propagation Letters, IEEE*; 1: 196-199, 2002.
- [12] Holloway CL, DeLyser RR, German RF, McKenna P, Kanda M. Comparison of electromagnetic absorber used in anechoic and semi-anechoic chambers for emissions and immunity testing of digital devices. *IEEE T Electromagn C*;39(1):33-47, 1997.
- [13] Naito Y, Anzai H, Mizumoto T. Design of super wideband electromagnetic wave absorber and its characteristics. *Electr Commun Jpn*;78(2):1-9, 2007.

- [14] Piao D, Li Y, Lu G. Broadband electromagnetic absorber designs using genetic algorithm. *IEEE Automation Congress, WAC 2008*.
- [15] Kong L, Yin X, Ye F, Li Q, Zhang L, Cheng L. Electromagnetic wave absorption properties of ZnO-based materials modified with ZnAl₂O₄ nanograins. *J Phys Chem C*;117(5):2135-46, 2013.
- [16] Xu Y, Zhang D, Cai J, Yuan L, Zhang W. Microwave absorbing property of silicone rubber composites with added carbonyl iron particles and graphite platelet. *J Magn Magn Mater*;327:82-6, 2013.
- [17] Zhang T, Huang D, Yang Y, Kang F, Gu J. Fe₃O₄/carbon composite nanofiber absorber with enhanced microwave absorption performance. *Mat Sci Eng B – Solid*;178(1):1-9, 2013.
- [18] Gradoni G, Micheli D, Moglie F, Mariani Primiani V. Absorbing cross section in reverberation chamber: experimental and numerical results. *Prog Electromagn Res B*;45:187-202, 2012.
- [19] Zhang W, Xu Y, Yuan L, Cai J, Zhang D. Microwave absorption and shielding property of composites with FeSiAl and carbonous material as filler. *J Mater Sci Technol*;28(10):913-9, 2012.
- [20] Micheli D, Pastore R, Gradoni G, Marchetti M. Tunable nanostructured composite with built-in metallic wire-grid electrode. *AIP Advances*;3:112132, 2013.
- [21] Micheli D, Apollo C, Pastore R, Bueno Morles R, Coluzzi P, Marchetti M. Temperature, atomic oxygen and outgassing effects on dielectric parameters and electrical properties of nanostructured composite carbon-based materials. *Acta Astronaut*;76:127-35, 2012.
- [22] Belaabed B, Wojkiewicz JL, Lamouri S, El Kamchi N, Lasri T. Synthesis and characterization of hybrid conducting composites based on polyaniline/magnetite fillers with improved microwave absorption properties. *J Alloy Compd*;527:137-44, 2012.
- [23] El Hasnaoui M, Triki A, Graca MPF, Achour ME, Costa LC, Arous M. Electrical conductivity studies on carbon black loaded ethylene butylacrylate polymer composites. *Esevier, J Non-Cryst Solids*;358(20):2810-15, 2012.
- [24] Emerson W. Electromagnetic wave absorbers and anechoic chambers through the years. *IEEE T Antenn Propag*;21(4):484-90, 1973.
- [25] Liu G, Wang L, Chen G, Hua S, Ge C, Zhang H, et al. Enhanced electromagnetic absorption properties of carbon nanotubes and zinc oxide whisker microwave absorber. *J Alloy Compd*;514:183-8, 2012.
- [26] Hou C, Li T, Zhao T, Zhang W, Cheng Y. Electromagnetic wave absorbing properties of carbon nanotubes doped rare metal/pure carbon nanotubes double-layer polymer composites. *Mater Design*; 33(1):413-8, 2012.
- [27] de Castro Folgueras L, Cerqueira Rezende M. Multilayer radar absorbing material processing by using polymeric nonwoven and conducting polymer. *Mat Res*;11(3):245-9, 2008.
- [28] Micheli D, Apollo C, Pastore R, Bueno Morles R, Laurenzi S, Marchetti M. Nanostructured composite materials for electromagnetic interference shielding applications. *Acta Astronaut*; 69(9-10):747-57, 2011.
- [29] Cui S, Weile DS. Application of a parallel particle swarm optimization scheme to the design of electromagnetic absorbers. *IEEE T Antenn Propag*;53(11):3616-24, 2005.
- [30] Cui, Weile DS, Volakis JL. Novel planar electromagnetic absorber designs using genetic algorithms. *IEEE T Antenn Propag*;54(6):1811-7, 2006.
- [31] Cui S, Weile DS. Robust design of absorbers using genetic algorithms and the finite element-boundary integral method. *IEEE T Antenn Propag*;51(12):3249-58, 2003.
- [32] Gradoni G, Micheli D, Mariani Primiani V, Moglie F, Marchetti M. Determination of the electrical conductivity of carbon/carbon at high microwave frequencies. *Carbon*;54:76-85, 2013.
- [33] Chen M, Zhu Y, Pan Y, Kou H, Xu H, Guo J. Gradient multilayer structural design of CNT/SiO₂ composites for improving microwave absorbing properties. *Mater Design*;32(5):3013-6, 2011.
- [34] Micheli D, Apollo C, Pastore R, Bueno Morles R, Laurenzi S, Marchetti M. Nanostructured composite materials for electromagnetic interference shielding applications. *Acta Astronaut*;69(9-10):747-57, 2011.
- [35] Micheli D, Apollo C, Pastore R, Marchetti M. X-band microwave characterization of carbon-based nanocomposite material, absorption capability comparison and RAS design simulation. *Compos Sci Technol*;70(2):400-9, 2010.
- [36] Micheli D, Apollo C, Pastore R, Bueno Morles R, Marchetti M, Gradoni G. *Electromagnetic Characterization of Composite Materials and Microwave Absorbing Modeling*. In: Reddy B, editor. *Advances in Nanocomposites - Synthesis, Characterization and Industrial Applications*, Rijeka, Croatia; InTech Open Access Publisher: 359-384, 2011.
- [37] Micheli D. *Radar Absorbing Materials and Microwave Shielding Structure Design: By using Multilayer Composite Materials, Nanomaterials and Evolutionary Computation*. Saarbrücken, Deutschland; LAP Lambert Academic Publishing: 334-446, 2012.
- [38] Micheli D, Pastore R, Gradoni G, Mariani Primiani V, Moglie F, Marchetti M. Reduction of satellite electromagnetic scattering by carbon nanostructured multilayers. *Acta Astronaut*; 88:61-73, 2013.
- [39] Micheli D, Pastore R, Apollo C, Marchetti M, Gradoni G, Mariani Primiani V, Moglie F. Broadband electromagnetic absorbers using carbon nanostructure-based composites. *IEEE T Microw Theory*; 59(10):2633-46, 2011.
- [40] Micheli D, Apollo C, Pastore R, Marchetti M. Modeling of microwave absorbing structure using winning particle optimization applied on electrically

conductive nanostructured composite material. *19th International Conference on Electrical Machines, ICEM 2010*.

- [41] Micheli D, Pastore R, Marchetti M, Gradoni G, Moglie F, Mariani Primiani V. Modeling and measuring of microwave absorbing and shielding nanostructured materials. *International Symposium on Electromagnetic Compatibility, IEEE EMC Europe 2012*.
- [42] Micheli D, Apollo C, Pastore R, Barbera D, Bueno Morles R, Marchetti M, et al. Optimization of multilayer shields made of composite nanostructured materials. *IEEE T Electromagn C*;54(1):60-9, 2012.
- [43] D Micheli, A Vricella, R Pastore, M Marchetti. Synthesis and electromagnetic characterization of frequency selective radar absorbing materials using carbon nanopowders. *Carbon 2014*, in press, <http://dx.doi.org/10.1016/j.carbon.2014.05.080> - available online 5 June 2014.

Contact Author Email Address

The contact author email address is:
davide.micheli@uniroma1.it

Copyright Statement

The authors confirm that they, and/or their company or organization, hold copyright on all of the original material included in this paper. The authors also confirm that they have obtained permission, from the copyright holder of any third party material included in this paper, to publish it as part of their paper. The authors confirm that they give permission, or have obtained permission from the copyright holder of this paper, for the publication and distribution of this paper as part of the ICAS 2014 proceedings or as individual off-prints from the proceedings.